

Signature current of SO₂-induced bronchitis in rabbit.

N Iwase, T Sasaki, S Shimura, T Fushimi, H Okayama, H Hoshi, T Irokawa, K Sasamori, K Takahashi, K Shirato

J Clin Invest. 1997;**99**(7):1651-1661. <https://doi.org/10.1172/JCI119328>.

Research Article

To investigate abnormalities of airway epithelial ion transport underlying chronic inflammatory airway diseases, we performed electrophysiological, histological, and molecular biological experiments using rabbits exposed to SO₂ as a model of bronchitis. By comparison with control, the SO₂-exposed trachea exhibited decreased short circuit current (I_{sc}) and conductance associated with increased potential difference. In normal trachea, apical ATP induced a transient I_{sc} activation followed by a suppression, whereas the bronchitis model exhibited a prolonged activation without suppression. This pathological ATP response was abolished by diphenylamine 2-carboxylate or Cl⁻-free bath solution. A significant increase in net Cl⁻ flux toward the lumen was observed after ATP in our bronchitis model. Isoproterenol or adenosine evoked a sustained I_{sc} increase in SO₂-exposed, but not in normal, tracheas. The Northern blot analysis showed a strong expression of cystic fibrosis transmembrane conductance regulator (CFTR) mRNA in SO₂-exposed epithelium. The immunohistochemical study revealed a positive label of CFTR on cells located lumenally only in SO₂-exposed rabbits. We concluded that the prolonged ATP response in our bronchitis model was of a superimposed normal and adenosine-activated current. The latter current was also activated by isoproterenol and appeared as a signature current for the bronchitis model airway. This was likely mediated by CFTR expressed in the course of chronic inflammation.

Find the latest version:

<https://jci.me/119328/pdf>



Signature Current of SO₂-induced Bronchitis in Rabbit

Nobuhisa Iwase, Tsukasa Sasaki, Sanae Shimura, Toshiaki Fushimi, Hiroshi Okayama, Hiroki Hoshi, Toshiya Irokawa, Kan Sasamori, Koichi Takahashi,* and Kunio Shirato

First Department of Internal Medicine, Tohoku University School of Medicine, Sendai; and *Central Research Laboratories, S.S. Pharmaceutical Co., Ltd., Chiba, Japan

Abstract

To investigate abnormalities of airway epithelial ion transport underlying chronic inflammatory airway diseases, we performed electrophysiological, histological, and molecular biological experiments using rabbits exposed to SO₂ as a model of bronchitis. By comparison with control, the SO₂-exposed trachea exhibited decreased short circuit current (Isc) and conductance associated with increased potential difference. In normal trachea, apical ATP induced a transient Isc activation followed by a suppression, whereas the bronchitis model exhibited a prolonged activation without suppression. This pathological ATP response was abolished by diphenylamine 2-carboxylate or Cl⁻-free bath solution. A significant increase in net Cl⁻ flux toward the lumen was observed after ATP in our bronchitis model. Isoproterenol or adenosine evoked a sustained Isc increase in SO₂-exposed, but not in normal, tracheas. The Northern blot analysis showed a strong expression of cystic fibrosis transmembrane conductance regulator (CFTR) mRNA in SO₂-exposed epithelium. The immunohistochemical study revealed a positive label of CFTR on cells located lumenally only in SO₂-exposed rabbits. We concluded that the prolonged ATP response in our bronchitis model was of a superimposed normal and adenosine-activated current. The latter current was also activated by isoproterenol and appeared as a signature current for the bronchitis model airway. This was likely mediated by CFTR expressed in the course of chronic inflammation. (*J. Clin. Invest.* 1997. 99:1651–1661.) Key words: ion transport • airway epithelium • bronchitis • cystic fibrosis transmembrane conductance regulator • ATP

Introduction

Cystic fibrosis (CF)¹ airway, known by its repetitive, intractable airway infections, has a causative relationship with a

defective epithelial Cl⁻ channel, the cystic fibrosis transmembrane conductance regulator (CFTR) (1). As with CF, bronchial obstruction by airway hypersecretion is also the most common pathological failure of chronic inflammatory pulmonary diseases including chronic bronchitis, bronchiectasis, and bronchial asthma. Along with mucus hypersecretion, certain pathological alterations in airway epithelial ion transport may therefore contribute to these chronic pulmonary diseases as they do in CF airway. The acute effects of various inflammatory mediators or pathogens on normal epithelia have been investigated in vitro, e.g., tumor necrosis factor attenuated an isoproterenol-evoked chloride (Cl⁻) current without altering baseline values (2), and a cell wall component of *Pseudomonas aeruginosa* depressed short circuit current (Isc) due to decreased Na⁺ absorption and Cl⁻ flux (3), whereas substance P (4) and eosinophil major basic protein (5) stimulated net Cl⁻ secretion across canine airway epithelia. Although there have been many reports concerning the morphological and/or mechanical alterations in airways of animal models of bronchitis exposed in vivo to sulfur dioxide (SO₂) (6–8), tobacco smoke (9), or ozone (10), apart from CF epithelia, information about the ion transport mechanism in such diseased airway epithelia as in chronic bronchitis, for example, is quite limited. The available papers, although small in number, suggest that there exist some alterations not only in the morphological but also in the bioelectric properties of pathological airway epithelia. For instance, the transepithelial electric potential difference (PD) was measured in vivo in human trachea (11), and smokers' airway was revealed to have a lower (less negative) PD when compared with an age-matched control group. In contrast, guinea pig airway exposed to ozone showed a higher ex vivo PD than that of normal animals (12). Nevertheless, these studies indicate that the baseline bioelectric properties are affected in pathological airways. Therefore, it is likely that there may also be some changes in the electrophysiological responsiveness to agents that are known to affect epithelial ion transport. To our knowledge, however, there have not been any reports so far describing qualitative alterations in triggered electrolyte transport in diseased airway epithelia.

To address this issue, we used an SO₂-exposed rabbit as a model for bronchitic airway, because the bioelectric properties of rabbit trachea have been well characterized (13, 14) and, also, because the methodology for preparing a bronchitic rabbit has been adequately established (15). Moreover, rabbit trachea has several advantages as a model for epithelial ion transport. As shown previously, airway submucosal glands secrete Cl⁻ in response to agonists such as acetylcholine, phenylephrine, and extracellular ATP (16, 17). Since rabbit airway has essentially no submucosal glands (18), we can exclude the possible contributions of these glands to Isc across airway epithelium in the presence of secretagogues. Furthermore, rabbit tracheal epithelium is primarily absorptive, a characteristic that is similar to that of human (13, 14, 19).

Address correspondence to Kunio Shirato, M.D., Professor and Chairman, First Department of Internal Medicine, Tohoku University School of Medicine, 1-1, Seiryomachi, Aoba-ku, Sendai 980-77, Japan. Phone: 81-22-717-7153; FAX: 81-22-717-7156.

Received for publication 25 July 1996 and accepted in revised form 23 January 1997.

1. Abbreviations used in this paper: A-aDO₂, alveolar-arterial PO₂ difference; ADO, adenosine; CF, cystic fibrosis; CFTR, cystic fibrosis transmembrane conductance regulator; G, electric conductance; I_{BE}, current unique for bronchitis model epithelium; Isc, short circuit current; ISO, isoproterenol; PD, potential difference.

J. Clin. Invest.

© The American Society for Clinical Investigation, Inc.

0021-9738/97/04/1651/11 \$2.00

Volume 99, Number 7, April 1997, 1651–1661

On the other hand, this type of epithelium has been shown to have no Isc response to β -agonists or agents that raise cellular cyclic adenosine 3',5'-monophosphate (cAMP) (13, 14, 19), although it possesses β -adrenergic receptors as well as an ability to increase the cellular level of cAMP in the presence of epinephrine, isoproterenol, or forskolin (20, 21). The electric refractoriness of the freshly isolated rabbit trachea to isoproterenol and other cAMP-mediated agents was also confirmed in our previous study, and extracellular ATP was found to elicit a transient increase in Isc that was carried by Cl^- , probably via P_{2u} -receptor (22).

Extracellular nucleotides or their derivatives are among the promising candidates as therapeutic agents for CF airway (23) because they stimulate Cl^- secretion through a path independent of CFTR, a cAMP-dependent Cl^- channel that is defective in CF epithelia. Moreover, the release of nucleotides and nucleosides by PMN inflammatory cells has been implicated to play a central role in the ion-transport response to PMN-dominated inflammatory responses in model systems of human gut epithelia (24). Accordingly, we examined the effects of extracellular ATP on freshly isolated trachea of SO_2 -exposed bronchitic rabbits using a short circuit technique. We here report that the tracheal epithelium from a rabbit model of bronchitis generated a unique current in response to exogenous ATP. Furthermore, the bronchitic epithelium was shown to carry Cl^- in response to isoproterenol and adenosine, a phenomenon that was absent in normal tissues. This is the first report that shows a distinctive electrophysiological signature of bronchitic epithelium.

Methods

SO₂ bronchitis model. Adult male New Zealand White rabbits weighing 1.8–2.4 kg were used. Rabbits were exposed to SO_2 gas 2 h/d, 5 d/wk for 5–7 wk according to the physical status (see below) of individual animals in an exposure apparatus with a modification of an earlier publication (15). The SO_2 gas concentration in the chamber was monitored with a sensor devised to measure 10–300 ppm of SO_2 by a color change of tetramethyl-*p*-diaminophenyl methane (15). The exposure regimen was as follows. We exposed 50–100 ppm SO_2 for the first week and raised it to 100–200 ppm during the second week, and thereafter increased the concentration to 200–300 ppm for several weeks. Rabbits began to develop cough after 4 wk of exposure and were used for experiments when they showed expectoration and/or weight loss of > 300 g due to poor feeding. The clinical symptoms of rhinorrhea, sneezing, cough, expectoration, and weight loss were reversible and recovered within 2 wk after stopping exposure. Therefore, we used the animals within 3 d after the exposure period. This study was approved by the Animal Care and Use Committee of the Tohoku University School of Medicine. The care and handling of the animals were performed in accordance with National Institutes of Health guidelines for the care and handling of animals (25).

Arterial blood gas analysis. In some rabbits, blood samples were drawn from an ear artery before anesthesia and analyzed by a blood gas analyzer (IL 1304S; Instrumentation Laboratory Inc., Lexington, MA). An approximate value of alveolar-arterial PO_2 difference (A-a DO_2) was calculated as $149 - \text{PaCO}_2/0.85 - \text{PaO}_2$ (Torr).

Electric characterization of rabbit trachea. Tracheas were removed from each rabbit under anesthesia with 30 mg/kg of intravenous thiopental, cleared of adjacent tissues, and placed in oxygenated Krebs-Ringer bicarbonate (KRB) solution containing (mM): 125 NaCl, 5 KCl, 1.2 MgCl_2 , 1.0 CaCl_2 , 25 NaHCO_3 , 1.2 NaH_2PO_4 , and 11 glucose. In Cl^- -free experiments, Cl^- was removed and replaced with isomolar gluconate. Tracheas were opened along the posterior membrane and cut into four segments and mounted on Ussing type cham-

bers. In some animals, the tracheal epithelial layer was peeled off using microscissors and microforceps under stereomicroscope and used for Northern blot analysis as described below. The Ussing chamber was 10 ml in volume with an exposed area of 0.5 cm^2 and bathed with KRB solution at 37°C, gassed with 95% O_2 /5% CO_2 at pH 7.4. The KRB solution in the chambers was circulated by the driving pressure of the gas which mixed the added agents uniformly in the KRB solution. We used two pairs of agar bridges filled with 3% agar in 3 M KCl solution. The PD across the tissue was measured with a pair of bridges placed 3 mm from either side of the tissue, and was always referenced to the submucosal solution. The liquid junction potential was nullified using the amplifier circuitry (CEZ-9100; Nihon Kohden Co., Tokyo, Japan). The other end was connected to the amplifier via a calomel half cell. A second pair of bridges was placed 3 cm from either side of the tissue, the fluid resistance between which was compensated using the amplifier circuitry before mounting the tissues. This pair of electrodes was used to pass sufficient current across the tissue to bring the PD to zero. This Isc is equivalent to the sum of electrogenic transepithelial active ion movements. Before initiating the experiments, the mounted tissue was allowed to equilibrate with the circuit open. Baseline PD (in mV) was evaluated at the point in which the value attained a plateau, usually 20–40 min after mounting. The baseline Isc (in $\mu\text{A}/\text{cm}^2$) was determined at ~ 20 min after clamping the voltage at 0 mV. The electric conductance (G, in mS/cm^2) was estimated from the change in current by applying voltage pulses of -2 or -3 mV at 0.5- or 3-min intervals.

Flux study. $^{22}\text{Na}^+$ and $^{36}\text{Cl}^-$ (5 μCi (185 kBq) each; Amersham Life Science, Buckinghamshire, United Kingdom) were added to either the mucosal or submucosal solution after electric parameters had stabilized. After a 30-min period for isotope equilibration under short circuit condition, sink samples (1 ml) were obtained every 15 min and replaced by an equal volume of cold KRB solution. After three sampling periods, ATP (10^{-4} M) was added to the mucosal solution and ~ 15 min was allowed for establishing the steady state level of Isc. Additional samples were then obtained three times at 15-min intervals to examine the effect of ATP on electrolyte fluxes. Samples were counted after the addition of liquid scintillant (Atomlight; Packard Instruments Co., Inc., Meriden, CT) in a liquid scintillation counter (Beckman LS6500; Beckman Instruments, Inc., Fullerton, CA). The peak energy of β -ray for ^{22}Na and ^{36}Cl was set at 0.546 and 0.709 MeV, respectively, and an external quenched standard curve was prepared by a dilution series of double-labeled solutions of known radioactivities. The radiocounts (cpm) of ^{22}Na and ^{36}Cl in the experimental samples were corrected automatically to dpm by a built-in program using the standard curve. Unidirectional fluxes of Na^+ and Cl^- were calculated from a conventional equation (26), $J = V(C_2 - C_1)/(tP^*A)$, where J is the unidirectional flux, in $\mu\text{Eq}/\text{cm}^2/\text{h}$; V is the volume of the chamber (10 ml); C_2 and C_1 are the radioactivities in the second and first samples for the flux period (with adequate corrections for the replaced cold KRB), in dpm/ml; t is the time period of the measurement (0.25 h); P^* is the specific activity of the isotope in the bathing solution, in dpm/ μEq ; and A is the area of the epithelial tissue exposed to bathing fluids (0.5 cm^2). Net flux was calculated as $J_{\text{net}} = J_{m \rightarrow s} - J_{s \rightarrow m}$; where J_{net} is the net ion flux and m and s refer to the mucosal and the submucosal side of the membrane, respectively. All fluxes were performed under short-circuited conditions. The tissues were paired on the basis of DC conductance (< 25% difference).

Histologic studies. The excised tracheas were fixed with 10% formalin in phosphate buffer (pH 7.2). After dehydration with ethanol (90%, 100%), they were embedded in paraffin. Histologic sections were prepared and stained with hematoxylin and eosin or Eosinostain-Hansel® (Torii and Co. Ltd., Tokyo, Japan).

Immunohistochemical study. Tracheas from normal and SO_2 -exposed rabbits were fixed in periodate-lysine-paraformaldehyde at 4°C for 2 h. After washings in sucrose (10%, 15%, 20%)/phosphate-buffered saline, they were embedded in O.C.T. compound (Miles Laboratories, Naperville, IL) in liquid nitrogen and stored at -70°C until use. The staining was performed with the alkaline phosphatase

anti-alkaline phosphatase (APAAP) method (27). Cryostat sections (5 μm) were stained for CFTR using monoclonal mouse anti-human CFTR IgG antibodies specific to R-domain or to COOH terminus (Genzyme Corp., Cambridge, MA). The slides were incubated with the primary antibody (0.5 $\mu\text{g}/\text{ml}$) diluted in Tris-buffered saline (TBS, 0.05 M Tris, 0.15 M NaCl, pH 7.6). After overnight incubation at 4°C, the slides were incubated with anti-mouse immunoglobulin goat immunoglobulins (Dako Corp., Carpinteria, CA) diluted 40 times with TBS containing 1% bovine serum albumin (TBS/BSA) for 30 min at room temperature followed by an incubation with soluble complexes of alkaline phosphatase and mouse monoclonal anti-alkaline phosphatase (Dako Corp.) diluted 60 times with TBS/BSA for 30 min at room temperature. After repeating these procedures once more, slides were developed by exposure to substrate for 8 min with Fast red substrate system (Dako Corp.) according to the manufacturer's protocol, and counterstained with hematoxylin. As controls, slides were evaluated in the absence of the primary anti-human CFTR antibody or with an irrelevant primary mouse monoclonal antibody (anti-human CD8; Wako Pure Chemicals, Osaka, Japan).

RNA isolation and Northern blot analysis. Total RNA was isolated by lysing the cells in Isogene (Nippon Gene, Tokyo, Japan). Total RNA (20 μg) was electrophoresed on a 1% agarose gel containing formaldehyde and transferred to nylon membranes (Hybond N; Amersham Life Science). Hybridization was carried out in solution with a final concentration of 5 \times sodium sulfate phosphate EDTA buffer (SSPE), 5 \times Denhardt's solution, 0.5% SDS, 20 $\mu\text{g}/\text{ml}$ denatured salmon sperm DNA, and 5 $\times 10^5$ cpm/ml of ^{32}P -labeled CFTR cDNA probe for 14 h. After hybridization, the membrane was washed once in 2 \times SSPE/0.1% SDS, twice in 1 \times SSPE/0.1% SDS at room temperature for 10 min, and then once in 1 \times SSPE/0.1% SDS at 60°C for 15 min. Autoradiography was performed by exposing an RX film (Fuji Photo Film Co., Tokyo, Japan) to the washed membrane.

The probe for CFTR cDNA. cDNA probe was prepared by reverse transcription-polymerase chain reaction. RNA from pancreas of normal rabbit was isolated as described above. Total RNA (1 μg) was converted to first-strand cDNA with oligo-dT primer and reverse transcriptase (SUPERSCRIPTM Preamplification System; GIBCO BRL, Gaithersburg, MD) according to the supplier's instructions. A 1,168-bp CFTR cDNA fragment was amplified by PCR from the first-strand cDNA with a set of primers which were designed according to the published rabbit CFTR cDNA sequence (28). The primer se-

quences for the rabbit CFTR cDNA were 5'-TGCAAACATGGT-ATGACTCG-3' and 5'-GCCTCTCCCTGTTCTGAATCT-3'. One-hundredth of cDNA synthesis reaction volume was combined at a final volume of 20 μl for PCR amplification using primers and 0.5 U of *Taq* DNA polymerase (TaKaRa, Otsu, Japan). PCR was performed for 40 cycles, each cycle consisting of denaturation at 94°C (1 min), annealing at 54°C (1 min), and elongation at 72°C (3 min). To confirm the specificity, a 1,120-bp cDNA fragment was amplified by second PCR with an internal primer and a 1:5,000 dilution of the first PCR product as template. The primers for the second PCR were 5'-TGCAAACATGGTATGACTCG-3' and 5'-GATGCGTCCGAATCTTCTTC-3'. The PCR product of 1,120 bp was purified using QIAquickTM Gel Extraction kit (QIAGEN, Düsseldorf, Germany) according to the supplier's instructions. The cDNA fragments were labeled with ^{32}P using Multiprime DNA labeling system (Amersham Life Science) to generate the ^{32}P -labeled CFTR cDNA probe.

Reagents. Adenosine, adenosine-5'-triphosphate (ATP) disodium salt, (\pm)-isoproterenol hydrochloride, amiloride hydrochloride, uridine-5'-triphosphate (UTP) sodium salt, 3-isobutyl-1-methylxanthine (IBMX), 8-(4-chlorophenylthio)-adenosine 3':5'-cyclic monophosphate (cpt-cAMP), forskolin, α,β -methyleneadenosine 5'-diphosphate (AMP-CP), and ionomycin calcium salt were purchased from Sigma Chemical Co. (St. Louis, MO). Diphenylamine-2-carboxylic acid (DPC) and anti-human CD8 antibody were from Wako Pure Chemicals. Anti-human CFTR monoclonal antibodies were from Genzyme Corp.

Statistical analysis. The data are presented as mean \pm SEM. For mean comparisons, one-way ANOVA or unpaired two-tailed Student's *t* test was used, except where stated otherwise. When variances of the two groups were not uniform, Cochran-Cox test was used. Significance was accepted at $P < 0.05$. *n* refers to the number of experiments.

Results

Clinical and histological evaluations of SO₂-exposed rabbits. During exposure to 200–300 ppm SO₂, all rabbits developed cough, sneezing, nasal discharge, and sometimes cyanosis. Mucus hypersecretion was evident when the tracheas were opened for mounting in the chamber. Analysis of arterial

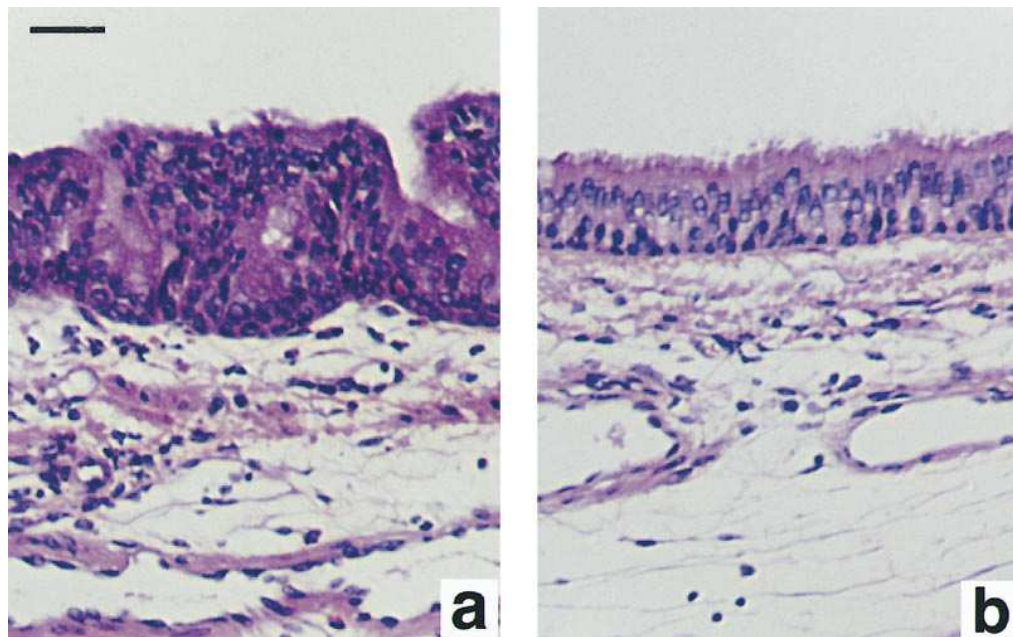


Figure 1. Light microscopic photographs of tracheas from rabbits exposed to SO₂ (a) or to filtered air (b). The tracheal sections from SO₂-exposed animals showed a loss of cilia, an infiltration of polymorphonuclear cells, and a thickened dysplastic epithelial layer. Both of the sections were obtained from a mid-portion of trachea with similar diameters. Hematoxylin and eosin stain. Bar, 100 μm .

Table I. Effects of Na⁺ Channel Blockade or Cl⁻ Deprivation on Baseline Parameters

		Amiloride		Cl ⁻ -free	
		Pre	Post	Pre	Post
Control	Isc (μA/cm ²)	90.3±9.4 (4)	51.9±4.0*	87.3±4.6 (5)	44.9±4.7‡
	PD (mV)	9.7±1.5	6.9±0.9‡	8.0±0.4	21.6±3.5§
	G (mS/cm ²)	9.6±0.7	7.7±0.5*	11.0±0.7	2.2±0.3*
SO ₂ -exposed	Isc	72.2±12.9 (5)	48.3±10.0‡	57.7±5.2 (9)	33.4±3.9§
	PD	24.6±3.9	18.4±2.6*	15.4±2.9	22.5±3.0§
	G	3.0±0.4	2.6±0.4*	4.4±0.6	1.5±0.1*

Effects of amiloride or Cl⁻ replacement on baseline electric properties in normal (control) and pathological (SO₂-exposed) epithelia. Pre and Post indicate values of pretreatment and posttreatment, respectively, by either agent. Note that the parameters in normal tissues bathed with Cl⁻-free solution were quite similar to those in bronchitis tissues in normal KRB solution. Statistical significance between the groups of pre- and posttreatment in this table was evaluated by paired *t* test (**P* < 0.05, †*P* < 0.01, §*P* < 0.001). Numbers in parentheses are the number of experiments.

blood gas showed significant hypoxemia compared with control animals, i.e., the values of PaO₂, PaCO₂, A-aDO₂ and pH for controls were 91.3±4.9, 38.2±2.1, 12.8±3.4, and 7.4±0.0, and for SO₂-exposed rabbits 57.7±4.2, 39.6±5.1, 44.8±4.4, and 7.4±0.1, respectively (*P* values were < 0.001, 0.810, < 0.001 and 0.963, respectively, *n* = 8 each). The A-aDO₂ values yielded a significant inverse correlation with transepithelial PD (*r* = -0.544, *P* = 0.0012, *n* = 31). Histologic examination revealed injury and partial loss of cilia, goblet cell hyperplasia, epithelial thickening, and infiltration of PMN into the submucosal and mucosal layer (Fig. 1). Almost all PMNs found in the present bronchitis specimens were considered to be neutrophils because of negative eosinophil staining.

Baseline electrophysiological properties in SO₂-exposed epithelium. SO₂-exposed tracheas yielded a significantly higher (more negative) PD, a lower Isc, and a lower G than those of normal tissues, i.e., PD, Isc, and G values for SO₂-exposed tracheas were 25.4±1.1 mV, 62.3±2.0 μA/cm², and 3.3±0.2 mS/cm², respectively (*n* = 55) compared with those of normal tissues which were 10.1±0.2 mV, 81.0±1.8 μA/cm², and 10.0±0.2 mS/cm², respectively (*n* = 122) (*P* < 0.001 each). The relative

contributions of Na⁺ and Cl⁻ currents to the baseline Isc were estimated either by treatment with amiloride, an Na⁺ channel blocker (10⁻⁴ M) or in Cl⁻-free experiments (Table I). In normal rabbits, the amiloride-sensitive fraction of the baseline Isc was 41.5±4.4% (*n* = 4), whereas that of the Cl⁻-free was 48.8±4.9% (*n* = 5). The SO₂-exposed tracheas showed similar relative contributions, i.e., 34.3±3.6% (*n* = 5) was amiloride sensitive and 42.1±5.8% (*n* = 9) was sensitive to Cl⁻-deprivation. In the absence of Cl⁻, PD rose and G decreased significantly in both preparations (Table I). Basolateral applications of the K⁺ channel blockers quinidine (10⁻⁴ M, *n* = 4 in normal and 5 in bronchitis) or tetraethylammonium chloride (TEA, 10⁻³ M, *n* = 1 each) were without effects on the basic electric parameters.

Distinct patterns of Isc response to exogenous ATP. In normal tracheas, apically applied ATP (10⁻⁴ M) induced a transient increase in Isc (27.9±4.3 μA/cm² above baseline) followed by a sustained suppression below the baseline (-22.8±4.0 μA/cm², *n* = 8) (see Fig. 2), which was associated with decreased electric conductance (Table II). We reported previously that the initial activation of Isc was carried mainly by Cl⁻

Table II. Changes in Isc and G in Responses Triggered by Various Agents in Normal and SO₂-exposed Tissues

		ATP		UTP		ISO		ADO	
		ΔIsc	ΔG	ΔIsc	ΔG	ΔIsc	ΔG	ΔIsc	ΔG
		μA/cm ²	mS/cm ²						
Normal	1 min	27.9±4.3 * (8)	-1.2±0.3 ‡	23.0±5.2 ‡ (6)	-1.8±0.6 §	-0.6±0.6 (4)	0.5±0.5	3.7±1.3 (3)	0.1±0.1
	15-20 min	-22.8±4.0 *	-1.7±0.5 §	-26.1±4.4 ‡	-3.0±0.9 §	-4.8±1.8	1.3±0.5	0.5±0.8	-0.0±0.3
SO ₂ -exposed	1 min	30.6±4.7 * (8)	0.8±0.2 ‡	17.6±1.1 * (7)	0.3±1.1	4.2±2.9 (5)	0.1±0.1	5.5±0.9 ‡ (4)	0.2±0.0 §
	15-20 min	16.3±3.9 ‡	0.5±0.2 §	0.2±2.0	-0.0±0.1	19.2±2.2 *	0.5±0.1 *	10.9±3.4 §	0.3±0.1 §

Changes in Isc and G in responses triggered by various agents in normal and SO₂-exposed tissues. Values were measured at time points immediately after the initiations of responses (1 min) and at the end of the experiments (15 to 20 min). Data are expressed as changes (Δ) from baseline. Comparison was made with the prior baseline value as a control by paired *t* test (§*P* < 0.05, †*P* < 0.01, **P* < 0.001). Numbers in parentheses are the numbers of experiments. ISO, isoproterenol; ADO, adenosine.

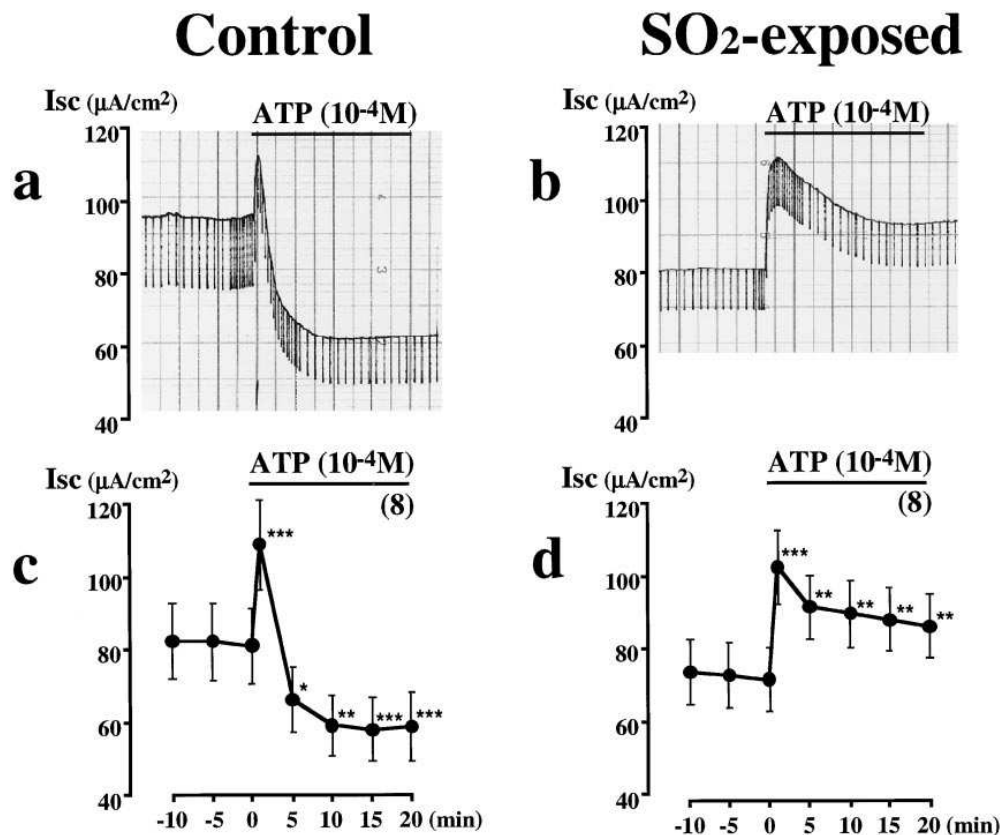


Figure 2. Distinctive ATP current activated in SO₂-exposed epithelium. Original recordings of I_{sc} in tracheas from control (a) and SO₂-exposed (b) animals. Tracheas from bronchitis model rabbit responded to exogenous luminal ATP in a dramatically different pattern in I_{sc} from those of normal control. Normal tracheas showed a transient increase followed by a marked depression in I_{sc} that was associated with a decrease in G, whereas tracheas exposed to SO₂ exhibited a prolonged activation of I_{sc} associated with a significant increase in G. The length of vertical lines imposed on I_{sc} recordings denotes an electric conductance at the time point of the tissue. The lower panels (c and d) show means ± SEM of eight experiments, respectively. Asterisks indicate significant differences compared with baseline values before ATP treatment (**P* < 0.05, ***P* < 0.01, ****P* < 0.001). Numbers in parentheses are the numbers of experiments.

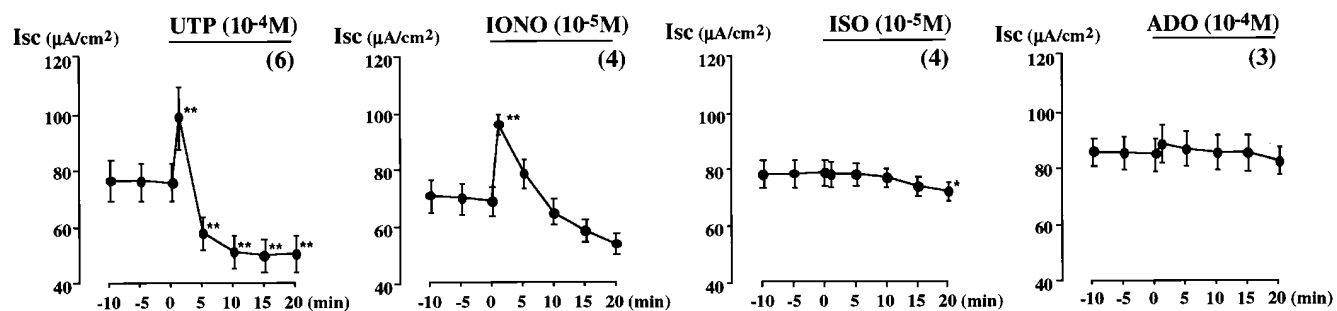
and the following suppression was due, at least in part, to a decrease in Na⁺ conductance (22). Luminal UTP (10⁻⁴ M, *n* = 6) and ionomycin (a calcium ionophore, 10⁻⁵ M, *n* = 4) showed qualitatively the same I_{sc} responses as ATP (see Fig. 3). In contrast, the SO₂-exposed epithelia exerted a sustained I_{sc} increase in the presence of ATP without suppression, which was in striking contrast to the normal response (Fig. 2 and Table II). This was associated with a significant increase in G. Luminal UTP (10⁻⁴ M, *n* = 7) caused a transient activation of I_{sc} followed by a return to the baseline value, while ionomycin (10⁻⁵ M, *n* = 4) showed a pattern similar to that in normal tissues (see Fig. 3).

Differential effects of cAMP-mediated agents on both preparations. To investigate the underlying mechanism of the ATP-induced sustained activation of I_{sc} in SO₂-exposed airway, we compared the effects of the β-adrenergic agonist isoproterenol (ISO) and adenosine (ADO), an ATP metabolite, on the two groups of trachea. In normal tissues, both ISO (10⁻⁵ M, *n* = 4) and ADO (10⁻⁴ M, *n* = 3) caused little, if any, alterations in the bioelectric parameters (Fig. 3 and Table II). Neither the phosphodiesterase inhibitor, 3-isobutyl-1-methylxanthine (IBMX, 10⁻³ M, *n* = 3), a membrane-permeable cAMP analogue 8-(4-chlorophenylthio)-adenosine 3':5'-cyclic monophosphate (cpt-cAMP, 10⁻⁴ M, *n* = 2), nor a stimulant of adenylyl cyclase forskolin (10⁻⁵ M, *n* = 3) induced any significant responses in normal tissues. This electric refractoriness of rabbit tracheas to β-adrenergic agonists or forskolin has been documented (13, 14, 19, 22). Surprisingly, however, in SO₂-bronchitis rabbit trachea, both ISO (*n* = 5) and ADO (*n* = 4) caused a significant increase in I_{sc} associated with increased

electric conductance (Fig. 3 and Table II). The newly discovered ISO- and ADO-evoked currents in SO₂-exposed epithelium were very similar to each other in time course and in magnitude (Fig. 3 and Table II). ISO and ADO are known to share a common cellular signaling pathway via cAMP. Ca²⁺ was considered not to be involved in the current of bronchitis model since ionomycin affected tracheas from both groups in the same way (Fig. 3). Therefore, we assumed that the ISO- and ADO-induced currents unique for this bronchitis model were evoked by a common cellular mechanism, which is described tentatively as I_{BE} in this paper, which means a current unique for bronchitis model epithelium.

Effect of AMP-CP on ATP-induced currents. Extracellular catabolism of ATP into ADP, AMP, or ADO is known to be carried out by a ubiquitous ectoenzyme, ecto-5'-nucleotidase (29). It might well be inferred that the ATP applied apically in this study was degraded to ADO, which in turn resulted in elevated cellular cAMP via adenosine A₂-receptors, thereby evoking I_{BE}. To test this hypothesis, we examined the effect of α,β-methyleneadenosine 5'-diphosphate (AMP-CP, 3 × 10⁻⁴ M), an inhibitor of ectonucleotidase (30), on the ATP-induced currents. As shown in Fig. 4 b, I_{BE} was abolished in the presence of AMP-CP and the bronchitis model epithelium nearly recovered its normal ATP response (*n* = 3), although the suppression after the initial activation was weak. The AMP-CP-treated SO₂-bronchitis tissues still responded to ADO. Moreover, a combined application of UTP and ADO reconstituted the bronchitic ATP response (*n* = 3, data not shown). In control tissues, AMP-CP itself caused no apparent alterations in baseline I_{sc} as well as in the ATP-evoked current (*n* = 4).

Control



SO₂-exposed

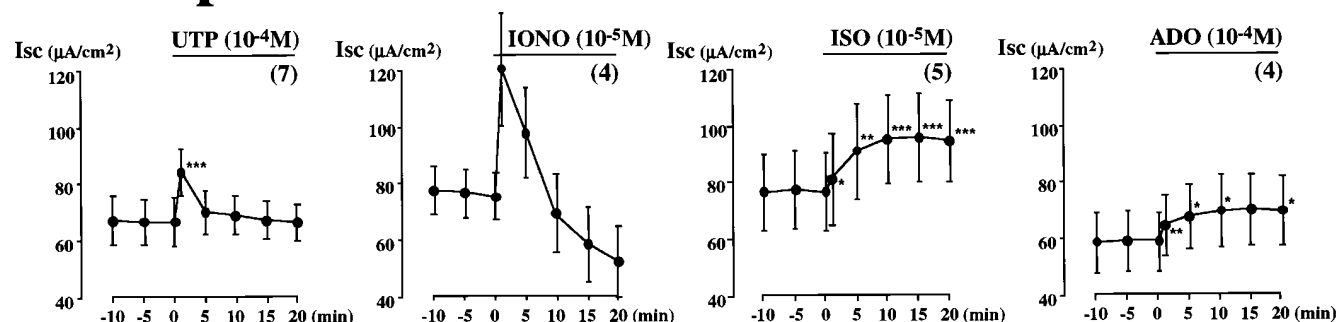


Figure 3. Comparisons of Isc responses triggered by various agents in normal and SO₂-exposed tissues. Tracheas from bronchitis model animals acquired responsiveness to ISO and ADO which was absent in control tissues. Data were expressed as means ± SEM. Asterisks indicate significant differences from baseline currents (**P* < 0.05, ***P* < 0.01, ****P* < 0.001). Numbers in parentheses are the numbers of experiments.

Specification of the ion species carrying I_{BE}. As shown in Fig. 4 c, amiloride failed to affect the ATP-induced current in bronchitis model (*n* = 3), while a major portion of the current was abolished in the presence of diphenylamine 2-carboxylic acid (DPC, 5 × 10⁻⁴ M), a nonspecific Cl⁻ channel blocker (to 18.6 ± 4.0% of bronchitic control values measured at 10 min af-

ter ATP application, *n* = 3) (Fig. 4 d). When Cl⁻ in the bathing solution was replaced by gluconate, the baseline current was decreased to ~ 60% of that of the bronchitic control value (Table I). Furthermore, a significant fraction of the ATP- or ISO-induced currents was abolished in the absence of Cl⁻ as shown in Fig. 5.

Table III. Pre- and Post-ATP Steady State Na⁺ and Cl⁻ Fluxes in Normal and SO₂-exposed Tracheas

Electric properties		Isc	G				
		μA/cm ²	mS/cm ²				
	Control	92.5 ± 9.1	6.8 ± 0.45				
	SO ₂ -exposed	48.4 ± 4.2	2.7 ± 0.4				
Ion fluxes (μEq/cm ² /h)		J ^{m→s} Na ⁺	J ^{s→m} Na ⁺	J ^{net} Na ⁺	J ^{m→s} Cl ⁻	J ^{s→m} Cl ⁻	J ^{net} Cl ⁻
Baseline	Control	2.38 ± 0.11	0.80 ± 0.07	1.58 ± 0.14	4.96 ± 0.41	6.55 ± 0.67	-1.62 ± 0.49
	SO ₂ -exposed	1.63 ± 0.14*	0.66 ± 0.08	0.95 ± 0.17 [‡]	2.54 ± 0.14 [§]	3.45 ± 0.14 [‡]	-0.94 ± 0.13
After ATP	Control	1.52 ± 0.13	0.57 ± 0.03	1.00 ± 0.10	4.26 ± 0.37	5.50 ± 0.69	-1.32 ± 0.42
	SO ₂ -exposed	1.61 ± 0.45	0.48 ± 0.36	1.15 ± 0.56	2.16 ± 0.33	3.96 ± 0.32	-1.58 ± 0.24 [¶]

Bioelectric properties and ion flux across excised rabbit trachea under short circuit condition. The top of the table shows the electric parameters of the tracheas used for the flux study (*n* = 10, each). The bottom of the table shows unidirectional and net fluxes obtained from control and SO₂-exposed tissue. $J_{net} = J_{m \rightarrow s} - J_{s \rightarrow m}$. After ATP denotes a steady state Isc after 15 min or later of ATP application. Statistical differences compared with respective control value ([‡]*P* < 0.05, **P* < 0.01, [§]*P* < 0.001); comparison with corresponding pretreatment value in the group ([¶]*P* < 0.05, ^{||}*P* < 0.001).

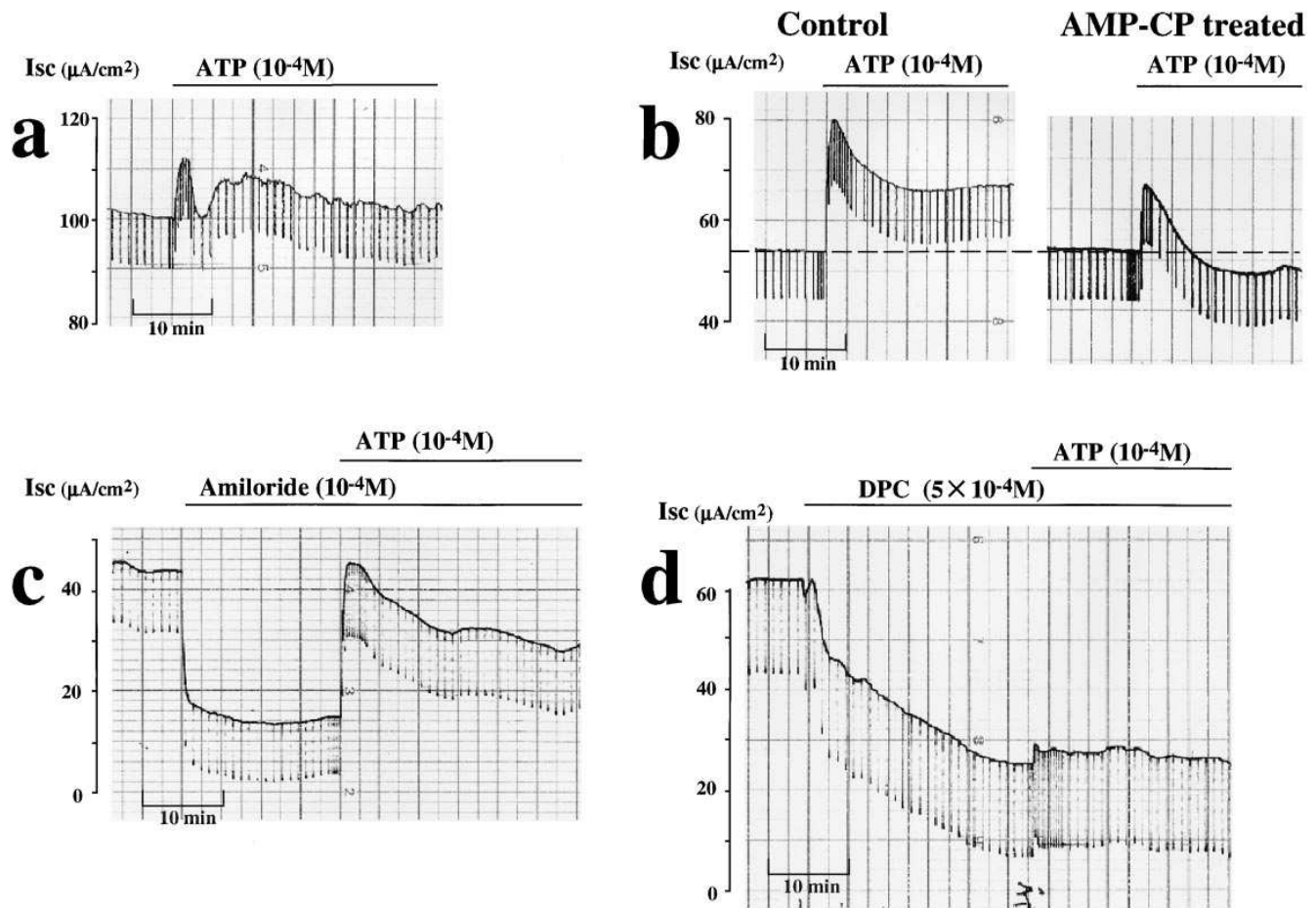


Figure 4. Original representative recordings of I_{sc} responses in SO_2 -exposed epithelia. (a) ATP induced a biphasic current response in this experiment, which suggested that at least two cellular mechanisms were underlying the pathological ATP response. (b) Effect of AMP-CP on ATP-induced current in SO_2 -exposed trachea. The inhibitor of ectonucleotidase abolished the second-phase current evoked by ATP in SO_2 -exposed tissues. (c) Effect of amiloride on ATP-induced current. The baseline current was decreased markedly in the presence of luminal amiloride, whereas the ATP response was not disturbed by amiloride. (d) Effect of DPC on ATP-induced current. DPC attenuated both the baseline current and the ATP response.

Flux study. To further characterize the altered electrophysiological properties in SO_2 -exposed trachea, a flux study was carried out using radioactive $^{22}Na^+$ and $^{36}Cl^-$ under short-circuit conditions. We measured flows of Na^+ and Cl^- in basal (resting) and in the steady state I_{sc} level after luminal ATP application, and compared normal and SO_2 -exposed tracheas. The results are summarized in Table III. The data showed clearly that the net flux of Na^+ ($J_{Na^+}^{net}$) in control tissue was reduced after ATP treatment (from 1.58 to 1.00 $\mu Eq/cm^2/h$, $P < 0.01$) without any significant alteration in Cl^- fluxes. In contrast, the baseline $J_{Na^+}^{net}$ in the pathological trachea (0.95 $\mu Eq/cm^2/h$) was smaller than that of control tissues (1.58 $\mu Eq/cm^2/h$, $P < 0.05$), and no further suppression was observed after ATP exposure. $J_{Cl^-}^{net}$ in baseline tended to be suppressed in SO_2 -exposed trachea (-1.62 vs. -0.94 $\mu Eq/cm^2/h$), but ATP increased it significantly, which was in good agreement with the electrophysiological observations. The SO_2 -exposed tissues were revealed to have a significantly lower basal Cl^- flux in passive direction (from mucosa to submucosa, 2.54 $\mu Eq/cm^2/h$) compared with that of control (4.96 $\mu Eq/cm^2/h$, $P < 0.001$) while the passive movement of Na^+ (from submucosa to mucosa) was unchanged (0.80 vs. 0.66, NS).

Immunohistochemical study using mAb against CFTR. A major fraction of I_{BE} was carried by Cl^- , and its pathway was likely to have been activated by intracellular cAMP since both ISO and ADO were equally effective. The only cAMP-stimulating Cl^- pathway identified so far in airway epithelia is CFTR. Therefore, we performed immunohistochemical staining of rabbit tracheal specimens using monoclonal antibody against CFTR. As shown in Fig. 6, a positive red stain was detected on the apical side of the cells which were located lumenally (Fig. 6 d), whereas the normal epithelium showed a negative stain (Fig. 6 b). Interestingly, the epithelial cells at the most distal trachea, where the damage due to SO_2 exposure was minimal as evidenced by the only slightly damaged cilia, showed a diffuse positive staining throughout the cytosol (Fig. 6 f).

Northern blot analysis for CFTR mRNA. To strengthen the present findings of immunohistochemistry for CFTR protein present in SO_2 -exposed epithelium, Northern blot analysis was carried out using isolated epithelial cells from normal and SO_2 -exposed tracheas (one normal and two SO_2 -exposed animals). As shown in Fig. 7, the normal intact epithelium showed little, if any, expression of CFTR mRNA, which was consistent with

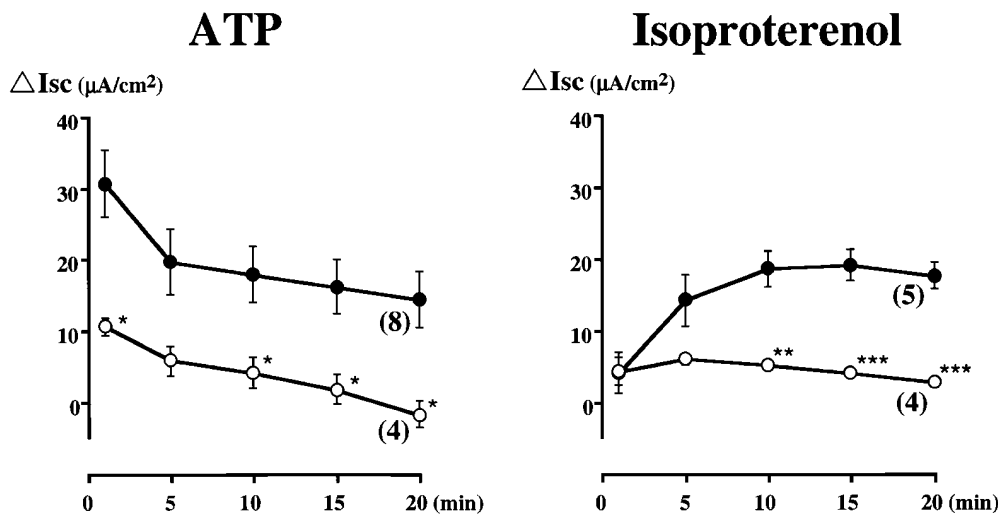


Figure 5. Effect of Cl^- -free bathing solution on ATP- and ISO-induced currents in SO_2 -exposed airway. Removal of Cl^- attenuated the responses significantly. Closed circles, responses in normal KRB solution; open circles, in Cl^- -free bathing solution. Asterisks denote significant differences between the two groups (* $P < 0.05$, ** $P < 0.01$, *** $P < 0.001$).

the observation of others (28). On the other hand, the mRNA was expressed strongly in SO_2 -exposed epithelial cells.

Discussion

Prolonged exposure of rabbits to high concentrations of SO_2 gas resulted in the clinical signs and pathophysiological changes in the respiratory tract consistent with those observed in humans with chronic bronchitis. We found that the value of A- aDO_2 was a useful predictor of the extent of the alteration in epithelial ion transport. The significant hypoxia and increase in A- aDO_2 in the present results may reflect a local shunt blood flow at the distal alveolar region due to bronchitis and/or mucus plugging, because the SO_2 -induced bronchitis is reversible both in function and morphology (6, 15), and the alveoli is reported to be histologically intact during SO_2 exposure (8). The rabbit pathological trachea shares common morphological characteristics with other animal models of SO_2 -exposed bronchitis (6–8) except that mucus gland hypertrophy or the mucus gland itself is absent in the rabbit model. Although a quantitative study was not performed, one of the most prominent features noted in the SO_2 -exposed rabbit was a thickening of the airway epithelium (Fig. 1). According to a detailed morphometric study using SO_2 -bronchitis dogs (6), the mean epithelial thickness more than doubled at all airway levels compared with that of control dogs, which is compatible with our and other's observations (8).

We found that the SO_2 exposure had a profound effect on the basic epithelial electric characteristics. A high PD, a low I_{sc} , and a markedly reduced G in the SO_2 -exposed rabbits had a striking similarity with the electrophysiological properties shown in the Cl^- -replacement study (Table I) and also with those in CF airway (31). Therefore, we considered that the bioelectric alterations in SO_2 -exposed airway might be explained by the closure of active Cl^- conducting pathway(s). In fact, as shown in Table I, the absolute value of Cl^- current occupied in total I_{sc} was reduced from 42.4 in normal tissues to 24.3 $\mu A/cm^2$ in bronchitic models, as estimated based on the Cl^- -free experiments. However, this was also the case with Na^+ transport, i.e., the amiloride-sensitive current was reduced from 38.4 to 23.9 $\mu A/cm^2$ (Table I). Closure of luminal Na^+ channels is thought to hyperpolarize the apical membrane, re-

sulting in a reduction in PD (19), which contradicts the present results. Accordingly, a suppression of the active Cl^- movement may not be the sole basis of the present change of baseline electric parameters. It may be that the activation of basolateral K^+ conductance, which also induces an increase in PD, is not involved in the present electrical alterations, because basolateral quinidine or TEA was without effect. An additional possibility is an interference of the passive cellular Cl^- pathway due to the thickened epithelial layer produced through SO_2 exposure. A low in vitro PD observed in normal rabbit trachea has been explained by the existence of a passive Cl^- conductance through the epithelial cells (13), which forms a simple shunt of PD. If the thickened dysplastic epithelium, possibly produced by a hyperplasia of the basal cells (6), did block this Cl^- specific pathway, then the present results of the bronchitic change in basic parameters could be explained more reliably. This notion was supported by the flux study (Table III). Passive unidirectional flow, i.e., flow from mucosa to submucosa for Cl^- or that from submucosa to mucosa for Na^+ , is thought to parallel the partial ionic conductance (32). Accordingly, the significant decrease in the passive unidirectional flow of Cl^- ($J_{Cl^-}^{m \rightarrow s}$) in the present SO_2 -exposed trachea seemed to contribute mainly to the reduction in baseline electric conductance since $J_{Na^+}^{s \rightarrow m}$ was not significantly different between the two groups.

The SO_2 -exposed rabbit airway epithelium acquired a reactivity to exogenous β -agonist. Although cultured fetal and adult rabbit trachea were reported to respond to epinephrine via β -receptors (33), freshly isolated normal rabbit trachea has been shown to be unresponsive to several cAMP-mediated agents including ISO (13, 14, 22). The cellular mechanism of the present ISO-triggered current in SO_2 -exposed rabbit (I_{BE}) is considered to be involved also in the ATP-activated pathological response via ADO. As shown in Fig. 4a, we happened to observe a biphasic current response to ATP in a bronchitis model. The initial rapid rise followed by a gradual activation in I_{sc} strongly suggested that the typical ATP response in bronchitis model, as shown in Fig. 2b, was a mixture of the two current components. That is, the first phase was activated by the same mechanism as in the normal ATP response, which was followed by I_{BE} induced by ADO. This was supported by the experiment using AMP-CP, a nucleotidase inhibitor. The ubiquity of ectonucleotidase on cellular membranes has been

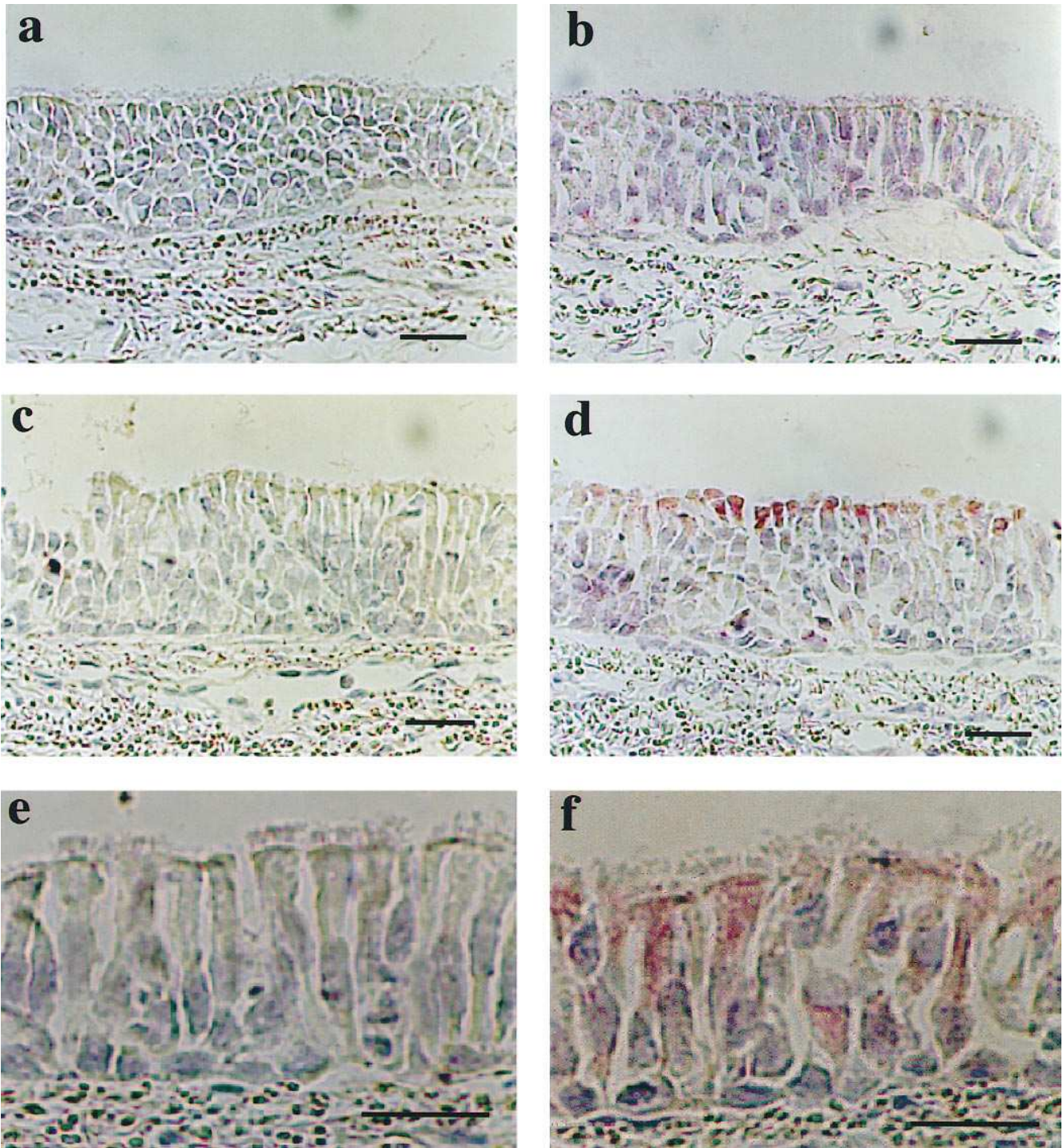


Figure 6. Immuno-alkaline phosphatase stain of tracheal mucosa using mouse antibody raised against human CFTR R-domain. Sections in *a–d* were from proximal trachea and *e* and *f* were from distal trachea. *a*, *b*, and *e* were tissues from normal animals, while *c*, *d*, and *f* were from bronchitis model animals. The left panels (*a*, *c*, and *e*) were without mAb against CFTR (negative control), while those in right panels (*b*, *d*, and *f*) were with CFTR antibody. As shown in *d*, the positive red stain was detected on the apical side of the cells located luminally, whereas the normal epithelium showed a negative stain (*b*). The epithelium at the most distal trachea with only slightly damaged cilia had diffuse positive staining throughout the cytosol (*f*). (Bar, 50 μm).

shown (29, 34) and the presence of adenosine receptors at the lumina was documented in human (35) and dog (36) airways. AMP-CP abolished the second phase current in SO_2 -exposed epithelium (Fig. 4 *b*). This resembled the bronchitic UTP response (Fig. 3) that showed a transient activation of I_{sc} with-

out I_{BE}, probably because the airway epithelium does not express receptors for UTP-metabolite uridine. It is of note that UTP exhibited a response without suppression in the bronchitis model (Fig. 3). In normal tissue, this suppression is attributable to a decreased Na^+ absorption as evidenced by the

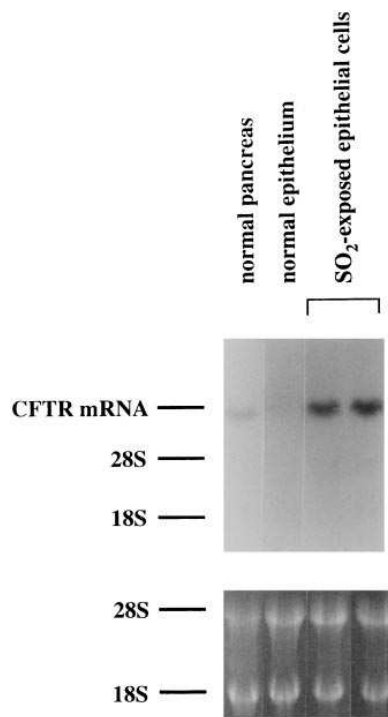


Figure 7. Northern blot analysis for CFTR mRNA. Total RNA (10 μ g) from each tissue was separated on formaldehyde gels and transferred onto a nylon membrane, which was hybridized with CFTR cDNA probe. The bottom of the figure shows the positions of the 28S and 18S rRNA bands on formaldehyde gels after ethidium bromide staining. CFTR mRNA was expressed little in normal intact epithelium. In contrast, the mRNA was strongly expressed in SO_2 -exposed epithelial cells.

present flux study (Table III) and our previous report (22). A similar finding was reported also in sheep trachea treated with acetylcholine (37). However, the underlying mechanism of the suppression of Na^+ absorption has not been established. It is also unclear why the bronchitis model epithelium lost the suppression. The high expression of CFTR in SO_2 -exposed epithelium (found in the present immunohistochemical and Northern blot analysis) may be related to this phenomenon. CFTR protein has been reported to regulate other channel types including epithelial Na^+ channel (38). Therefore, it is possible that, in the bronchitis model airway, the upregulated CFTR protein might downregulate, at least in part, the activity of the Na^+ channels. This may result in a weak suppression of Na^+ absorption subsequent to ATP treatment. In fact, the baseline $J_{\text{Na}^+}^{\text{net}}$ was significantly depressed in SO_2 -exposed tissue when compared with control and was left unchanged after ATP exposure (Table III).

There are some possible mechanisms underlying the activation of I_{BE} . In a recent investigation using rabbit epithelial cells in culture (39), nonciliated bronchiolar epithelial (Clara) cells were shown to generate a sustained Cl^- current that was stimulated by ISO. If the proliferated epithelial cells in the present study included a population similar to Clara cells, the I_{BE} could be attributed to its presence in the proximal airway. However, the major cell population reported to proliferate in bronchitis models appeared to be basal cells that are also present in normal airway (6). Additional information concerning the biological and electrophysiological behavior of Clara cells *in vivo* may be required to address this possibility. As an alternative explanation, the expression of I_{BE} may have resulted from *de novo* generation of several kinds of membrane receptors including adenosine- and β -adrenergic receptors in bronchitis model epithelium. However, this possibility is remote because the normal rabbit epithelium isolated from trachea already possesses abundant β -adrenergic receptors and generates cAMP in re-

sponse to ISO, epinephrine, or prostaglandin E_2 (20, 21). Therefore, we assumed that I_{BE} was evoked through a newly generated effector sensitive to a common cellular mechanism shared by ATP, ISO, and ADO. Cyclic AMP, then, is the most probable candidate for the second messenger operating under these situations, being raised via β_2 -adrenergic and adenosine A_2 receptors. In addition, the major portion of I_{BE} was carried by Cl^- , suggesting that CFTR was the effector.

The nucleotide base pair homology of rabbit CFTR to that of human in exons 7–11 was between 86 and 91% per exon, and the R-domain synthetic peptide was reported to have 78% homology with the human cDNA (28). On the basis of the striking similarity of human CFTR with rabbit, immunohistochemistry was conducted using commercially available monoclonal antibodies against human CFTR. As shown in Fig. 6, positive dense staining of a label of CFTR was found on cells located at the lumina in the proximal trachea (Fig. 6d) and a diffuse positive stain was recognized throughout the cytoplasm in the most distal trachea (Fig. 6f). This observation was further confirmed by Northern blot analysis, in which CFTR mRNA was upregulated strongly in the SO_2 -exposed epithelial cells (Fig. 7). This was unexpected because a series of investigations has shown unequivocally a downregulation of CFTR gene expression by an inflammatory agent. That is, one of the stimulants of protein kinase C (PKC) and airway irritants, phorbol myristate acetate (PMA), suppressed CFTR mRNA expression in T84 colon carcinoma cell line (40). Nevertheless, it is possible that an unknown mechanism coping with the action of PKC may get into operation *in vivo* in inflammatory airways such as bronchitis. In a report investigating a CF gene and protein expression during rabbit lung development, rabbit CFTR was recognized diffusely in the cytosol at 22 d of gestation and localized to the apical membrane at 29 d, but did not appear in adult rabbit (28). It is not surprising, therefore, that a dedifferentiation occurred to the epithelial cells proliferating in a chronic inflammatory environment, expressing the fetal epithelial phenotype containing CFTR and thus acquiring the responsiveness to cAMP-mediated agents.

In this study, we showed that SO_2 -induced bronchitic epithelium produced an altered responsiveness to exogenous apical ATP, isoproterenol, or adenosine. The newly emerged current in bronchitis model epithelium, I_{BE} , was carried mainly by Cl^- and was activated by cAMP-mediated agents. By immunohistochemical and Northern blot analyses, the involvement of CFTR, a cAMP-regulated Cl^- channel, is proposed as an underlying mechanism of the qualitative transformation in the triggered epithelial ion transport in SO_2 -exposed rabbit airway. Recently, in *Streptococcus pneumoniae*-infected rabbit airway, an upregulation of CFTR protein within the epithelial layer was reported by immunohistochemistry (41). This indicates that the upregulation of CFTR is not specific to SO_2 -induced bronchitis but occurs more generally in inflammatory airways. The current in SO_2 -exposed airway we identified may reflect a functional adaptation of inflammatory airways to flush out pathogens or irritants, thus possibly contributing to the airway hypersecretion together with the actions of various inflammatory mediators.

Acknowledgments

We gratefully acknowledge Ms. Kuniko Suzuki for technical assistance and Mr. Brent Bell for reading the manuscript.

This work was supported in part by grant-in-aid for scientific research from the Ministry of Education, Science and Culture of Japan.

References

1. Anderson, M.P., H.A. Berger, D.P. Rich, R.-J. Gregory, A.E. Smith, and M.J. Welsh. 1991. Demonstration that CFTR is a chloride channel by alteration of its anion selectivity. *Science (Wash. DC)*. 253:202–205.
2. Satoh, M., T. Sasaki, S. Shimura, H. Sasaki, and T. Takishima. 1991. Tumor necrosis factor attenuates β agonist-evoked Cl^- secretion in canine tracheal epithelium. *Respir. Physiol.* 84:379–387.
3. Stutts, M.J., J.H. Schwab, M.G. Chen, M.R. Knowles, and R.C. Boucher. 1986. Effects of *Pseudomonas aeruginosa* on bronchial epithelial ion transport. *Am. Rev. Respir. Dis.* 134:17–21.
4. Al-Bazzaz, F.J., J.G. Kelsey, and W.D. Kaage. 1985. Substance P stimulation of chloride secretion by canine tracheal mucosa. *Am. Rev. Respir. Dis.* 131: 86–89.
5. Jacoby, D.B., I.F. Ueki, J.H. Widdicombe, D.A. Loegering, G.J. Gleich, and J.A. Nadel. 1988. Effect of human eosinophil major basic protein on ion transport in dog tracheal epithelium. *Am. Rev. Respir. Dis.* 137:13–16.
6. Seltzer, J., P.D. Scanlon, J.M. Drazen, R.H. Ingram, Jr., and L. Reid. 1984. Morphologic correlation of physiologic changes caused by SO_2 -induced bronchitis in dogs: the role of inflammation. *Am. Rev. Respir. Dis.* 129:790–797.
7. Man, S.F.P., W.C. Hulbert, G. Man, K. Mok, and D.J. Williams. 1982. Effects of SO_2 -exposure on canine pulmonary epithelial functions. *Exp. Lung Res.* 15:181–198.
8. Killingworth, C.R., J.D. Paulauskis, and S.A. Shore. 1996. Substance P content and preprotachykinin gene-I mRNA expression in a rat model of chronic bronchitis. *Am. J. Respir. Cell Mol. Biol.* 14:334–340.
9. Jones, R., P. Bolduc, and L. Reid. 1973. Goblet cell glycoprotein and tracheal gland hypertrophy in rat airways: the effect of tobacco smoke with or without the anti-inflammatory agent phenylmethyl oxadiazole. *Br. J. Exp. Pathol.* 54:229–239.
10. Mariassay, A.T., W.M. Abraham, R.J. Phipps, M.W. Sielczak, and A. Wanner. 1990. Effect of ozone on the postnatal development of lamb mucociliary apparatus. *J. Appl. Physiol.* 68:2504–2510.
11. Knowles, M.R., W.H. Buntin, P.A. Bromberg, J.T. Gatzky, and R.C. Boucher. 1982. Measurements of transepithelial electric potential differences in the trachea and bronchi of human subjects *in vivo*. *Am. Rev. Respir. Dis.* 126: 108–112.
12. Stutts, M.J., and P.A. Bromberg. 1987. Effects of ozone on airway epithelial permeability and ion transport. *Toxicol. Lett.* 35:315–319.
13. Jarnigan, F., J.D. Davis, P.A. Bromberg, J.T. Gatzky, and R.C. Boucher. 1983. Bioelectric properties and ion transport of excised rabbit trachea. *J. Appl. Physiol.* 55:1884–1892.
14. Boucher, R.C., and J.T. Gatzky. 1983. Characteristics of sodium transport by excised rabbit trachea. *J. Appl. Physiol.* 55:1877–1883.
15. Kase, Y., H. Seo, Y. Oyama, M. Sakata, K. Tomoda, K. Takashima, T. Hitoshi, Y. Okano, and T. Miyata. 1982. A new method for evaluating mucolytic expectorant activity and its application. I. Methodology. *Arzneim.-Forsch./ Drug Res.* 32:368–373.
16. Sasaki, T., S. Shimura, M. Wakui, Y. Ohkawara, T. Takishima, and K. Mikoshiba. 1994. Apically localized IP_3 receptors control chloride current in airway gland acinar cells. *Am. J. Physiol.* 267:L152–L158.
17. Shimura, S., T. Sasaki, M. Nagaki, T. Takishima, and K. Shirato. 1994. Extracellular ATP regulation of feline tracheal submucosal gland secretion. *Am. J. Physiol.* 267:L159–L164.
18. Jeffery, P.K., and L. Reid. 1977. Ultrastructure of airway epithelium and submucosal gland during development. In *Development of the Lung*. (Lung Biol. Health Dis. Ser. Vol. 6). W.A. Hodson, editor. Dekker, New York. 87–134.
19. Boucher, R.C. 1994. Human airway ion transport. Part one. *Am. J. Respir. Crit. Care Med.* 150:271–281.
20. Liedke, C. 1986. Interaction of epinephrine with isolated rabbit tracheal epithelial cells. *Am. J. Physiol.* 251:C209–C215.
21. Maridini, I.A., N.C. Higgins, S. Zhou, J.L. Benovic, and S.G. Kelsen. 1994. Functional behavior of the β -adrenergic receptor-adenylyl cyclase system in rabbit airway epithelium. *Am. J. Respir. Cell Mol. Biol.* 11:287–295.
22. Iwase, N., T. Sasaki, S. Shimura, M. Nara, M. Yamamoto, S. Suzuki, and K. Shirato. 1995. ATP increased Cl^- secretion from non-ciliated epithelial cells and suppressed Na^+ absorption via a Ca^{2+} -mediated pathway in rabbit trachea. *Am. J. Respir. Crit. Care Med.* 151:183a. (Abstr.)
23. Knowles, M.R., L.L. Clarke, and R.C. Boucher. 1991. Activation by extracellular nucleotides of chloride secretion in the airway epithelia of patients with cystic fibrosis. *N. Engl. J. Med.* 325:533–538.
24. Madara, J.L., T.W. Patapoff, B. Gillece-Castro, S.P. Colgan, C.A. Paros, C. Delp, and R.J. Mrsny. 1993. 5'-Adenosine monophosphate is the neutrophil-derived paracrine factor that elicits chloride secretion from T84 intestinal epithelial cell monolayers. *J. Clin. Invest.* 91:2320–2325.
25. U.S. Department of Health and Human Services. 1985. Guide for the care and use of laboratory animals. NIH publication No. 86-23, revised 1985. U.S. Government Printing Office, Washington, DC.
26. Al-Bazzaz, F.J., and Q. Al-Awqati. 1979. Interaction between sodium and chloride transport in canine tracheal mucosa. *J. Appl. Physiol.* 46:111–119.
27. Hoshi, H., I. Ohno, M. Honma, Y. Tanno, K. Yamauchi, G. Tamura, and K. Shirato. 1995. IL-5, IL-8 and GM-CSF immunostaining of sputum cells in bronchial asthma and chronic bronchitis. *Clin. Exp. Allergy.* 25:720–728.
28. McGrath, S.A., A. Basu, and P.L. Zeitlin. 1993. Cystic fibrosis gene and protein expression during fetal lung development. *Am. J. Respir. Cell Mol. Biol.* 8:201–208.
29. Misumi, Y., O. Shigemori, S. Hirose, and Y. Ikehara. 1990. Primary structure of rat liver 5'-nucleotidase deduced from the cDNA. *J. Biol. Chem.* 265:2178–2183.
30. Bruns, R.F. 1990. Adenosine receptors. Roles and pharmacology. *Ann. NY Acad. Sci.* 603:211–226.
31. Cuthbert, A.W. 1989. Defects in epithelial ion transport in cystic fibrosis. In *Molecular Medicine. Cystic Fibrosis*. P. Goodfellow, editor. Oxford University Press, Oxford. 25–40.
32. Gatzky, J.T. 1975. Ion transport across the excised bullfrog lung. *Am. J. Physiol.* 228:1162–1171.
33. Zeitlin, P.A., G.M. Loughlin, and W.B. Guggino. 1988. Ion transport in cultured fetal and adult rabbit tracheal epithelia. *Am. J. Physiol.* 254:C691–C698.
34. Mo, M., S.G. Eskin, and W.P. Schilling. 1991. Flow-induced changes in Ca^{2+} signaling of vascular endothelial cells: effect of shear stress and ATP. *Am. J. Physiol.* 260:H1698–1707.
35. Cushley, M.J., A.E. Tattersfield, and S.T. Holgate. 1983. Inhaled adenosine and guanosine on airway resistance in normal and asthmatic subjects. *Br. J. Pharmacol.* 15:161–165.
36. Pratt, A.D., G. Clancy, and M.J. Welsh. 1986. Mucosal adenosine stimulates chloride secretion in canine tracheal epithelium. *Am. J. Physiol.* 251: C167–C174.
37. Acevedo, M. 1994. Effect of acetyl choline on ion transport in sheep tracheal epithelium. *Pflügers Arch.* 427:543–546.
38. Stutts, M.J., C.M. Canessa, J.C. Olsen, M. Hamrick, J.A. Cohn, B.C. Rossier, and R.C. Boucher. 1995. CFTR as a cAMP-dependent regulator of sodium channels. *Science (Wash. DC)*. 269:847–850.
39. Van Scott, M.R., C.M. Penland, C.A. Welch, and E. Lazarowski. 1995. β -Adrenergic regulation of Cl^- and HCO_3^- secretion by Clara cells. *Am. J. Respir. Cell Mol. Biol.* 13:344–351.
40. Trapnell, B.C., P.L. Zeitlin, C.-S. Chu, K. Yoshimura, H. Nakamura, W.B. Guggino, J. Bargon, T.C. Banks, W. Dalemans, A. Pavirani, et al. 1991. Down-regulation of cystic fibrosis gene mRNA transcript levels and induction of the cystic fibrosis chloride secretory phenotype in epithelial cells by phorbol ester. *J. Biol. Chem.* 266:10319–10323.
41. Elliot, W.M., N. Kartner, J.R. Riordan, and J.C. Hogg. 1996. Effect of airway inflammation on the expression of the CFTR protein in rabbits. *Am. J. Respir. Crit. Care Med.* 153:778a. (Abstr.)